Available online at www.sciencedirect.com

jmr&t Journal of Materials Research and Technology

journal homepage: www.elsevier.com/locate/jmrt

Original Article

Effects of laser-textured on rake face in turning PCD tools for Ti6Al4V

P. Fernández-Lucio [a,*], I. Villarón-Osorno [a], O. Pereira Neto [b], E. Ukar [a], L.N. López de Lacalle [b], A. Gil del Val [c]

[a] University of the Basque Country (UPV/EHU), Department of Mechanical Engineering, Plaza Torres de Quevedo s/n, 48013 Bilbao, Spain

[b] Aeronautics Advanced Manufacturing Centre (CFAA), University of the Basque Country (UPV/EHU), Zamudio, Spain

[c] Tecnalia, Basque Technology Research Alliance (BRTA), Parque Científico y Tecnológico de Gipuzkoa E20009 Donostia-San Sebastián, Spain

ARTICLE INFO

Article history:
Received 12 March 2021
Accepted 2 August 2021
Available online 6 August 2021

Keywords:
Ti6Al4V
PCD chipbreakers
Laser engraving

ABSTRACT

The demand inherent to the aeronautical industry in terms of productivity and quality requirements leads to develop new cutting tools. Hence, PCD tools meet the requirements in productivity while machining low machinability aeronautical alloys such as Ti6Al4V. Tool chipbreakers play a considerable role in terms of tool life. However, due to the extreme conditions (temperature and pressure) required to manufacture PCD tools, any complex geometry on tool rake faces is not viable, so chipbreakers are not possible, except for those external to inserts.

This work proposes a groove-type laser engraved chipbreaker design and a manufacturing methodology, with experimental validation on turning a Ti6Al4V workpiece. The so-manufactured chipbreakers achieve titanium alloy chip fragmentation, making easy chip removal from the cutting zone.

A set of experiments involving various laser parameters to characterize the PCD depth and surface integrity and experimental validation for those chipbreakers designs were carried out in finishing cutting conditions. The optimum parameters for the engraving of PCD were found, obtaining satisfactory breakage of titanium chips. Chip length was always below 17.29 mm.

1. Introduction

The aeronautical industry is one of the most demanding sectors [1] concerning quality and productivity. In particular, turbomachinery components need alloys that must be light and withstand high temperatures during their service life. These alloys take relevance in critical rotary components such as fans, compressors, and turbines [2]. Turning is one of the most used operations when manufacturing rotary turbomachinery components. Furthermore, most of the critical components of aero engines are made of low machinability alloys,

* Corresponding author.
E-mail address: pablo.fernandezd@ehu.eus (P. Fernández-Lucio).

https://doi.org/10.1016/j.jmrt.2021.08.004

which can be nickel-based [3], cobalt-based [4], and titanium-based [5], such as Inconel® 617, CoCrMo alloys, and Ti6Al4V respectively. Due to their excellent mechanical properties at high temperatures, these alloys present a challenge when turning to obtain the previously mentioned parts.

Several studies around turning processes regarding low machinability alloys have been carried out over recent years. Suárez et al., 2019 studied the influence of cutting forces in tool wear when machining Haynes® 282. The tests resulted in a non-visible relation of the cutting forces with tool wear [6]. Amigo et al., 2020 developed a roughness and force model which was validated with high feed turning tests. The model predicted fairly well both the resulting roughness and the cutting forces neglecting the effect of the nose of the tooltip radius, obtaining particularly good results when turning Haynes® 263 and Inconel® 718 [7]. Cooling is also a relevant variable in the turning process. Actually, various authors have studied the influence of cooling techniques when machining low machinability alloys. In those studies, it was concluded that certain combinations of cutting fluids are not always the best choice as it can be drawn from Amigo et al., 2020 [7] and Ganguli and Kapoor 2016 [8]. On the one hand, Ganguli and Kapoor 2016 reported an increase of 75% of the tool life when using an atomization-based cutting fluid. On the other hand, Amigo et al., 2020 concluded that the use of oil emulsion coolant enhanced the tool performance when machining Inconel® 718 whereas Haynes® 263 is presented as a viable niche to be opened for cryogenic cooling.

Titanium alloys [9] are typical in the cold zone of aero engines, in segments and components before the combustion chambers. These alloys are characterized by an excellent strength-to-weight ratio in combination with high corrosion resistance [10]. However, from a manufacturing point of view, its high chemical reactivity with cutting tools substrates on one hand, and its low thermal conductivity on the other, lead to a difficult machining process [11]. The most common microstructure of Ti6Al4V alloy, the alfa-beta microstructure, carbide inserts (WC grains sintered with cobalt binder) is the primary option. In this case, the diffusion effect between tool cobalt binder and Ti6Al4V is the predominant tool wear mechanism, causing a short tool life [12]. Particularly, when low cutting speed is applied, severe adhesive interaction between tool-chip takes place on the tool rake face, causing built-up edge formation (known as BUE) [13,14]. On the other hand, the cratering phenomenon appears after adhesion [15], or before it with poor coolant conditions or at high speeds.

One of the current research lines is providing WC inserts with coatings. Thus, TiN and TiAlN coatings are applied to improve tool cutting performance and reduce tool wear [16]. However, other advanced coatings were tested recently. For example, AlTiN coating is the most used industrially due to it presents at the same time resistance to high cutting stresses and temperatures combined with low diffusion wear [17], careful finishing of coating, and droplet elimination after PVD is very recommended [18]. Another coating applied to non-ferrous metals is those CrN-based [19]. In this case, the coating is characterized by presenting excellent resistance to corrosion and oxidation due to its low affinity to non-ferrous materials [20,21]. Although these coatings allow achieving higher tool life [22], an increase in cutting conditions is always needed to reduce manufacturing time; and the higher the cutting speed the lower the tool life.

Consequently, other advanced tool materials have been analysed to replace WC inserts. Some of them are ceramics. This substrate has good behaviour at high cutting temperatures and, therefore, allows increasing cutting speed as Fernández-Valdivielso et al., 2020 performed tests turning Austempered Ductile Iron (ADI). From the study, it can drown an excellent abrasion wear resistance behaviour presented by mixed ceramic tools [23]. In Da-Wang et al., 2018 research, several TiB_2–B_4C based ceramic tools were used for turning Ti6Al4V alloy at 150, 200, 250, and 300 m/min cutting speeds. The results showed that at 150 m/min a machined cutting length of 800 mm was achieved when a substrate of 20%–80% of B_4C–TiB_2 is used [24]. Other ceramics used applied for turning Ti6Al4V were studied by Da Silva et al., 2005. In this case, Al_2O_3 with 30% SiC was used at 140, 200, 400, and 500 m/min. The results showed that at 140 m/min 2.7 min of tool life was achieved [25]. In both cases, ceramic tools supposed an increase in cutting speed by nearly double compared to turning with WC inserts [26,27]. Nevertheless, in Da Silva et al., 2005 ceramic inserts were also compared with polycrystalline diamond (PCD) inserts. In the latter case, a tool life of 55 min was obtained, that is, 2100% more than the obtained with ceramic tools [25]. Therefore, the use of PCD tools implies not only an increase in cutting speed but also a drastic increase in tool life, obtaining a real productivity increase in turning processes. Consequently, the versatility of PCD tools allows a wide range of possibilities from non-ferrous material processing to micro finishing operations of low machinability materials due to the capability of producing different cutting edge sizes [28]. Regarding the tool wear mechanism, PCD is a substrate composed of diamond polycrystalline micro-grains in a cobalt binder, sintered together, and very hard. Then, despite being resistant to the abrasion phenomenon, the chemical affinity between the binder (Co) and Ti6Al4V happened in a similar way to WC tools. This issue was analysed in Sales et al., 2017, stating that crater wear is predominant tool wear due to the stick-slip connected with chips pluck out [29]. Similar results were obtained by Sadik et al., 2019. In this case, abrasion wear was reported as secondary wear mechanisms [30]. Finally, Oosthuizen et al., 2011 reported the diffusion of chips onto the tool cutting surface [31]. Therefore, to continue improving turning processes with PCD inserts, this issue must be taken into account.

One way to minimize these phenomena is the generation of chipbreakers on the inserts rake face. However, ceramics manufacturing and PCD sintering (and PCD plate brazing on carbide substrate) present problems to generate chipbreakers directly on tools rake face. In contrast to WC tools, in which chipbreakers are obtained during the sintering process using specific moulds, straight and reinforced ceramic tools are manufactured using Hot Isostatic Pressing (HIP), and these tools have to undergo temperatures at 1250–2000 °C range, under a pressure of 28–69 MPa in a vacuum of 1.3 MPa for an hour. This process allows the dispersion of the whiskers into the matrix [32]. Only simple geometries, such as buttons and square shapes, can be produced with flat faces. Therefore, a secondary process, such as laser marking or engraving or EBM or EDM, must manufacture the chipbreakers. This line of

research is currently being developed. Thus, Xing et al., 2014 proposed several texturizations with Nd: YAG laser on Al_2O_3/TiC ceramic inserts were carried out to deal with hardened steel. The results showed that cutting temperature between the insert and the workpiece material was provoked [33]. Analogue results were achieved by Cui et al., 2018. In this case, an intermittent turning performance of hardened AISI 52100 steel was carried out with several texturized patterns by a laser power of 3 W in Al_2O_3/(W, Ti)C ceramic tools, demonstrating that different kinds of textures could improve tool life [34]. On the other hand, in Rajbongshi et al., 2018, several texturizations were carried by Micro-EDM in WC inserts. The results when AISI D2 steel showed that not only tool life was increased but also cutting temperature and cutting forces were reduced [35]. Moreover, Mishra et al., 2018 made a textured WC tool by using a nanosecond fibre laser, which resulted in a texturization of the rake face of the insert, achieving a reduction in the cutting forces, thrust force, and tool flank wear [36]. Regarding PCD tools, in Wu et al., 2020 an adjustable chipbreaker was designed for turning Al7075-T651 aluminium alloy with PCD inserts. The system consisted of a structure clamped to the rake face of the tool, setting up an angle between this face and the active face of the chipbreaker. Moreover, a numerical model based on the FEM was developed to determine the optimal position of chipbreakers and the angle formed between the tool rake face and the active face of the chipbreaker. The results showed that chip breakability was improved [37]. Alagan et al., 2019 tried turning Alloy 718 with WC textured tools by means of laser ablation improving tool performance observing no crater or notch wear on the cutting tools [38]. Everson et al., 2009 analysed the effect on the microstructure of a laser processed PCD tool obtaining a satisfactory insert, although some drawbacks were addressed such as a recast layer and the formation of amorphous carbon due to the interaction of the laser input energy and the PCD tool [39]. Pacella et al., 2019 also found amorphous graphite when laser processing the PCD. Besides, enhancement of PCD hardness due to the local plastic deformation phenomena of stresses due to grain size and distribution was found [40]. Nevertheless, despite these researches advanced to obtain satisfactory chipbreakers based either on texturizations or by mechanical systems, they were not applied on PCD tools for turning Ti6Al4V alloys.

Therefore, the novelty of the work here presented is to propose groove-type chipbreakers in PCD inserts, which enhances chip breakability and consequently, reduces the chip-insert contact area for achieving the breakage of Ti6Al4V chip using finishing cutting conditions. For this purpose, this work was included the laser grooving characterization of PCD tool material with the aim of optimizing the process and finally, the chipbreakers proposed were validated in Ti6Al4V (aged state) turning at high speeds.

2. Laser grooving characterization

For the manufacturing of the textured tool, a Trumpf® Trumark 5000 station was used. This station is equipped with a pulsed Nd: YAG fibre laser of the average output power of 50 W. The pulse frequency range goes from 1 to 1000 kHz with a minimum pulse duration of 7 ns. The laser beam quality is characterized by an M^2 value of 1.6. The 2D scanner responsible for the beam movement in the XY plane has a 110 × 110 mm workspace, as can be seen in Fig. 1, and a laser spot size, when focused, of 50 μm. The maximum speed of the scanning unit is 10,000 mm s^{-1}. On the other hand, to obtain precise texturing on the rake face of the cutting insert, precise tooling for positioning the PCD insert was needed. Moreover, to focus the laser spot, the focal length is fixed and, thus, the tooling has to have precise dimensions.

Firstly, a characterization of the PCD was needed. Since as has been described by the authors previously [21], the milling mechanisms of each PCD depend on PCD grain size and distribution. The PCD is the cutting edge of an SNGA 120408 MD220 cutting insert, PCD grade with an average micro-grain size of 10 μm with 10–12% cobalt binder. To determine the best-suited parameters in order to establish the depth of the PCD milled when processed, a number of parameters were

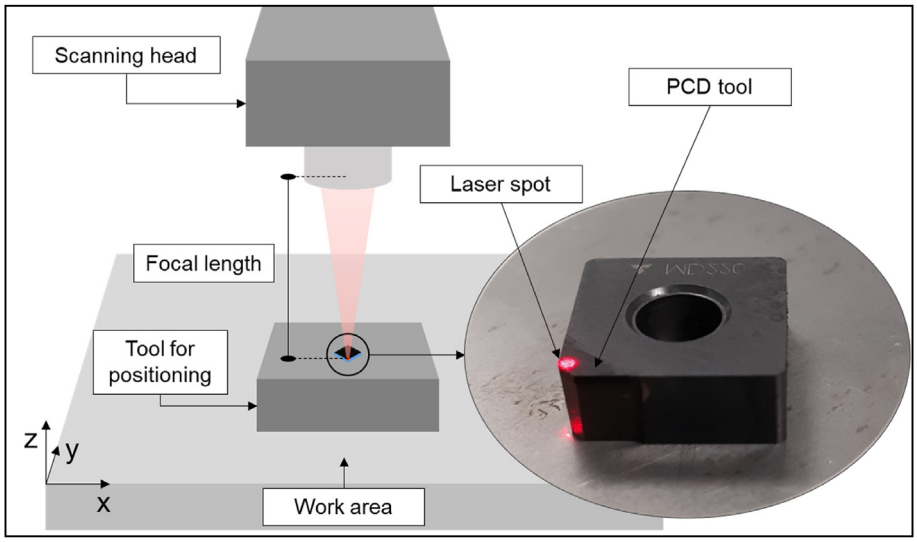

Fig. 1 – TruMark Station 5000 experimental setup and process detail.

established to be tested in a 1.5 × 1.5 mm square geometry. Topographical analyses were carried out with a Leica 3DCM confocal microscope equipped with up to ×150 focusing lens, capable of achieving resolutions of less than 2 nm when operating with the previously mentioned ×150 lens and with the option to apply a white or blue light.

In the mentioned topographical analysis, the surface quality of the bottom of the laser textured areas was studied. To do so, ISO 25178 norm was applied to obtain S_a, arithmetic mean deviation of surface topography, and S_z, the sum of the highest peak and the deepest valley of the surface topography, parameters. With these parameters, some surface defects such as recast layer very common in this kind of process can be detected. To that purpose first, the topography of the whole square was taken. After that, the bottom of the square is isolated since is the area which must be studied. Because the obtained data from the confocal microscope is not filtered, a Gaussian filter with a 0.8 mm cut-off length was applied.

A tendency of reduction of the roughness as the radial step gets smaller can be observed. Since the tracks of the laser are closer, the energy that arrives at the material is higher due to the overlap that is created. Considering the spot size of the laser of 50 μm and the Gaussian distribution of the energy coming from the laser when a 0.05 mm radial step is applied, there is no overlapping between tracks. In contrast, when a 0.02 mm radial step is applied, an overlap of approximately 50% is being applied, resulting in a higher energy input into the area, leading to a more efficient material removal ratio and a smoother engraved surface.

However, the downside is that an increment in process time is experienced due to the increment of tracks needed by the laser to cover the same surface. Therefore, those are the parameters used in the texturizations. Table 1 summarizes the obtained results for each test. Although values 6 and 18 present similar roughness, the parameters from test 18 allow higher productivity, and thus, resulting in the chosen parameter to manufacture the grooves. Fig. 2 shows the best four measurements (18, 6, 15, and 3) in terms of S_a and two intermediate measurements in terms of S_a and S_z (8 and 10). It is also included a detailed view of test 18 where it can be seen the quality of the final engraved surface.

Moreover, for a complete analysis, another set of experiments were set. On these tests, the evolution of the depth was analysed applying various numbers of Hatchings or repetitions represented in Table 2. The combination of laser parameters chosen corresponds to test number 18 since that parameter combination is to be used when engraving the PCD tools.

Fig. 3 represents the evolution of the depth of the abovementioned 1.5 × 1.5 mm square designed to characterize the PCD material. The material presents, when laser processed, a linear behaviour, meaning that an intuitive correlation between the numbers of hatchings necessary to increase a certain depth of the groove can be set.

3. Machining validation: experimental setup

Aiming at validating the laser grooving characterization, a battery of longitudinal turning tests in Ti6Al4V alloy was carried with several chipbreaker designs. In Table 2, the chemical composition and mechanical properties of the alloy used are shown.

All the tests were carried out in a CMZ TC25BTY turning centre with 35 kW of spindle power and integral spindle. Cutting forces were registered with a triaxial Kistler® 9192 A piezoelectric dynamometer and an OROS® OR35 real-time multi-analyser with a sampling frequency of 12,800 samples/s. The initial diameter of the workpiece was 130 mm with a length of 300 mm. In Fig. 4, the experimental setup is presented.

The inserts were SNGA 120408 MD220 provided by Zubiola Diamond Tool Solutions Coop® with a micro-grain of 10 μm with 10% cobalt as binder material. These inserts were modified to avoid the effects of the cutting-edge radius. This modification was carried out due to finishing cutting

Table 1 – Laser parameters combination and obtained roughness values.

Test Number	Scan Speed (mm/s)	Pulse frequency (Hz)	Radial step (mm)	Pulse duration (ns)	Measured S_a (μm)	Measured S_z (μm)
1	300	30,000	0.05	250	1.82	19.311
2	300	30,000	0.03	250	1.57	20.883
3	300	30,000	0.02	250	1.35	20.252
4	300	40,000	0.05	250	1.78	20.504
5	300	40,000	0.03	250	1.63	20.560
6	300	40,000	0.02	250	1.32	20.392
7	300	50,000	0.05	250	1.83	19.905
8	300	50,000	0.03	250	1.59	20.405
9	300	50,000	0.02	250	1.38	19.135
10	400	30,000	0.05	250	1.80	19.030
11	400	30,000	0.03	250	1.65	20.024
12	400	30,000	0.02	250	1.36	19.938
13	400	40,000	0.05	250	1.79	19.309
14	400	40,000	0.03	250	1.58	19.523
15	400	40,000	0.02	250	1.33	20.609
16	400	50,000	0.05	250	1.75	19.755
17	400	50,000	0.03	250	1.61	19.533
18	400	50,000	0.02	250	1.31	19.013

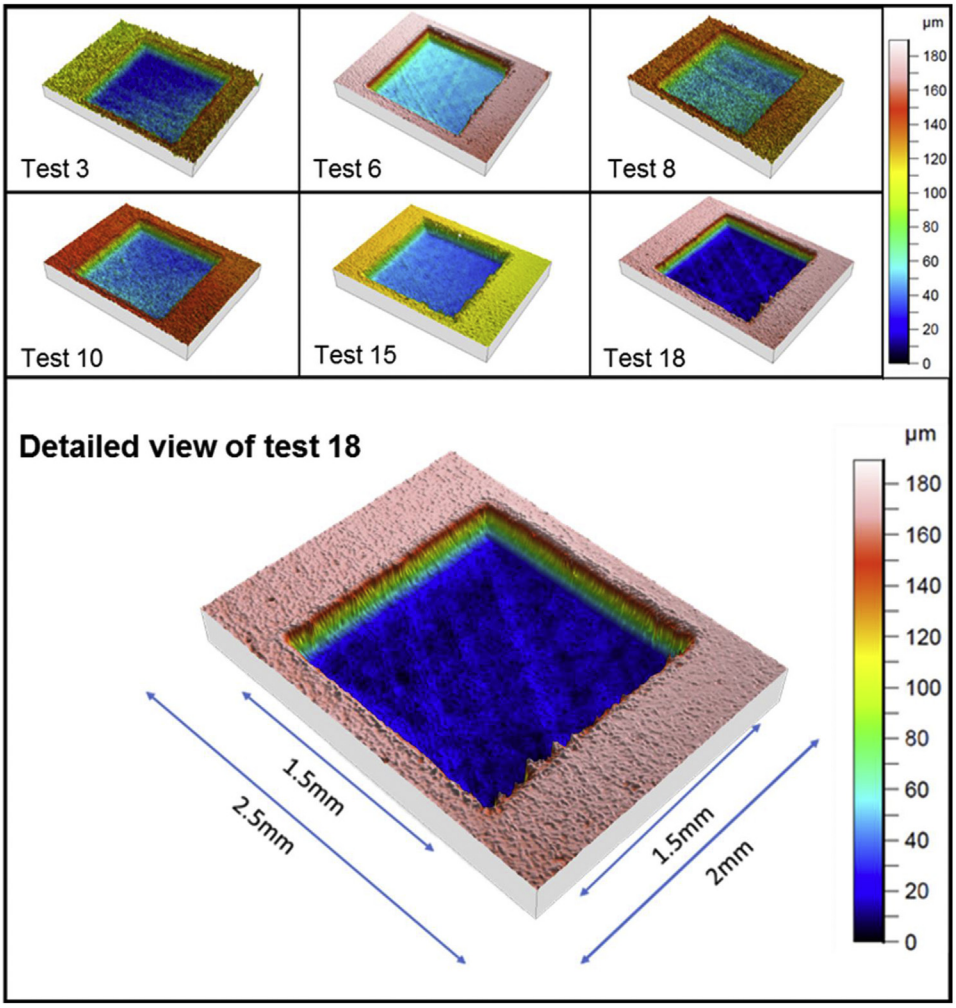

Fig. 2 – 3D view of some of the measured surfaces of the laser engraving PCD characterization design of experiments.

conditions were used. In particular, a cutting speed of 150 m/min, feed of 0.05 mm/rev. and depth of cut of 0.25 mm was used. These cutting conditions were obtained in a previous test to obtain severe conditions with the aim of enhancing the effect of tool wear mechanisms in the insert substrate. Each test was repeated three times. During the tests, a synthetic oil emulsion of 10% was injected at 6 bars.

To manufacture the grooves on the rake face of the tools, different parameters have to be taken into account: separation from the cutting edge, separation between each groove (s), groove width (w), groove depth (d), and angle with the cutting edge. All the textured tools were performed with the same dimensional parameters. Patel et al., 2020 stated that distance to cutting edge and groove depth is closely related to tool temperature: as they become higher, tool temperature increases [41]. As it is a finishing process, tool temperature must be controlled not to damage the final workpiece surface. Moreover, Kumar Mishra et al., 2020 stated that the distance to the cutting edge is critical to avoid catastrophic fracture of the tool [42]. Hence, the textures have been fabricated at a distance of 100 µm from the cutting edge with groove depth of 10 µm. The distance of the textures from the cutting edge has

Table 2 – Chemical composition and mechanical properties of tested Ti6Al4V.

Chemical Composition (%)							
Al	V	Fe	O	C	N	Y	Ti
6.50	4.17	0.24	0.17	0.01	<0.01	<0.0005	Balance

Mechanical Properties						
Hardness	Young's Modulus	Tensile Strength	Density	Specific Heat Capacity	Melting Temp.	Thermal Conduct.
36 HRC	114 GPa	883 MPa	4430 kg/m^3	526 J/(kg·K)	1650 K	6.70 W/(m·K)

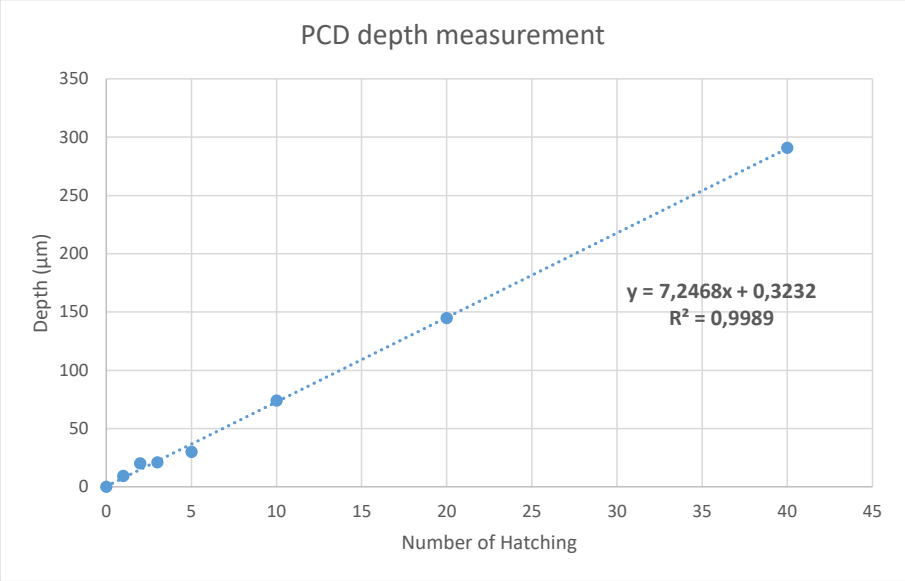

Fig. 3 – PCD depth measurement.

been kept to avoid high thermomechanical concentration at the cutting edge due to texturing and consequent tool edge fracture and chipping. According to Iqbal et al., 2009, with the cutting parameters used during tests (v_c of 150 m/min and f of 0.05 mm/rev), the chip-tool contact length exceed the distance of textures from the cutting edge. This design confirms that the chip underside contacts with the textured surface [43]. In the case of width of the grooves and separation between grooves, it was chosen 50 µm for both of them, except for the overlapped grooves in which the width was increased to

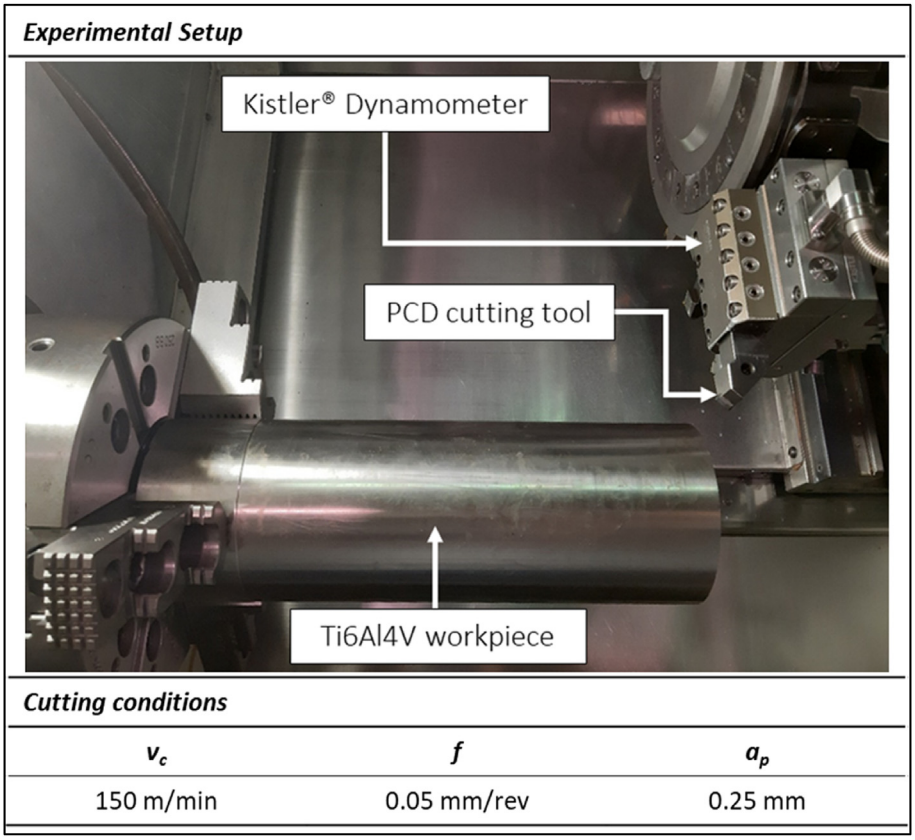

Fig. 4 – Experimental setup.

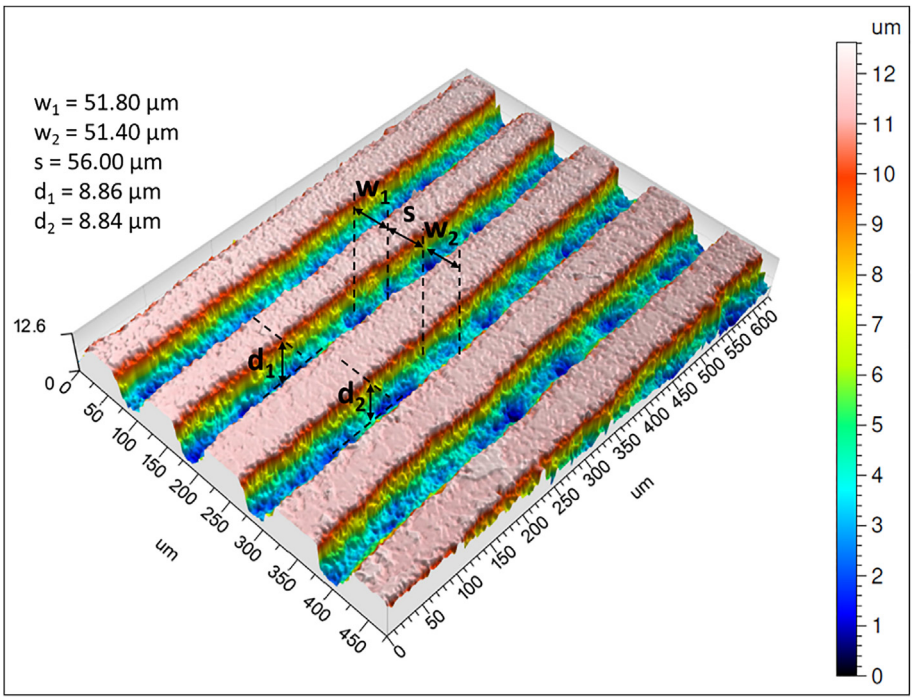

Fig. 5 – Topography of the manufactured grooves with their real dimensions.

100 µm. These values were selected due to the importance of a small increase of cutting forces to obtain the objective of breaking the chip since increasing groove width and separation minimize cutting forces [41].

The surface features on the tool grooved tooltip are presented in Fig. 5, is possible to observe the obtained groove parameters. Furthermore, it can be seen that there is no recast layer on the rake surface of the tool. Topography was measured by a confocal microscope Leica DCM3D.

Regarding chipbreakers design, five different textured surfaces were proposed in which several groove angles were applied. Concretely the angles, taking the cutting edge as a reference, proposed were 0°, 45°, 90°, a combination of 0° and 90° and an overlap texture of the parallel groove (0°). The reasons for proposing these angles were: grooves parallel to the cutting edge offer more resistance to chip flow increasing the chip breaking capacity; in the case of grooves perpendicular to the cutting edge, chip removal is encouraged reducing friction between the chip and the rake face of the cutting tool because they are in the direction of chip flow; grooves at 45° and in a combination of 0° and 90° with the cutting edge are an intermediate between the two previous ones; overlapped grooves in the direction of the cutting edge enhance the effect of breaking the chip.

Finally, the chip was collected after each test with the aim of verifying chipbreakers suitability in Ti6Al4V. The chipbreakers designs are shown in Fig. 6.

4. Machining validation: results & discussion

Chips obtained from the tests carried out are shown in Fig. 7. According to ISO 3685:1993 chip morphology classification, the

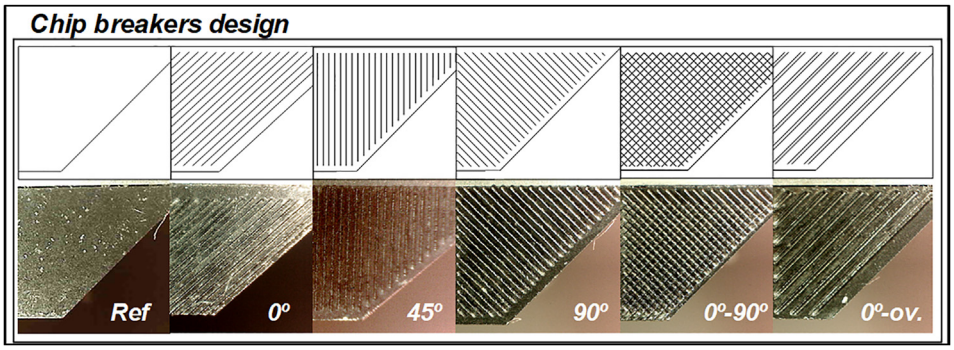

Fig. 6 – Chipbreakers designs.

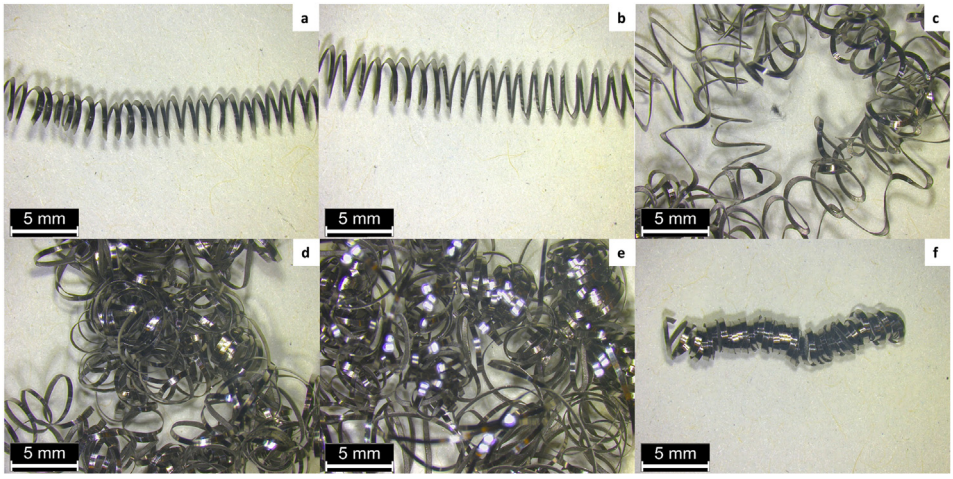

Fig. 7 – Chips morphology: (a) Reference, (b) 0°, (c) 45°, (d) 90°, (e) 0°–90° combination, (f) overlap.

reference insert generated a long washer-type helical chip. In the case of the inserts provided with chipbreakers, they were classified into three categories. Inserts with chipbreakers with 90° and its combination with 0° generated snarled washer-type helical chips. In the case of the insert with a chipbreaker at 0° and 45°, similar chips were obtained to the reference one. Finally, the chipbreaker with 0° overlapped caused short conical helical chips.

Taking into account the importance of breaking the resulting chip, that classification can be divided as follows: acceptable chips, which break facilitating the evacuation, and unacceptable chips that do not break [44]. Considering this, in the resulting chips from the test carried out in this work, the reference insert and the chipbreakers applied at 0° and 45°, respectively, chips flowed in a similar way. In particular, chips went away from the workpiece and in the opposite direction of the feed, helping to evacuate chips without damaging the machined surface. On the other hand, chips resulting from inserts provided with grooves perpendicular to the cutting edge (90°) and with the combination of parallel and perpendicular grooves (0°–90°) were tangled with the workpiece due to the redirection of the chip flow. This resulted in a scratched final surface, which becomes an issue for finishing operations. Finally, when the chipbreaker with 0° overlapped is applied to the insert, the chips flow is similar to the obtained with the reference insert and the inserts provided with chipbreakers with 0° and 45°, respectively. However, in this case, chips obtained are smaller due to the effect achieved by this chipbreaker in which chips did not present more than 17.29 mm of length. This fact highlights the importance of chipbreaker depth to face a suitable way in which chips cannot flow through an obstacle and, therefore, break.

Chips obtained are closely related to cutting forces results. Hence, in Fig. 8, the average of binormal force (F_b), tangential

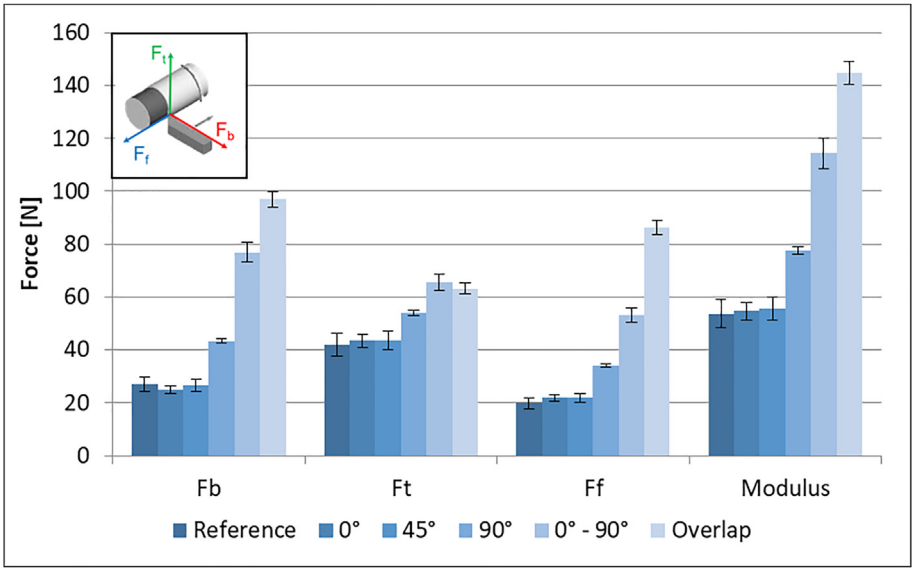

Fig. 8 – Average cutting forces.

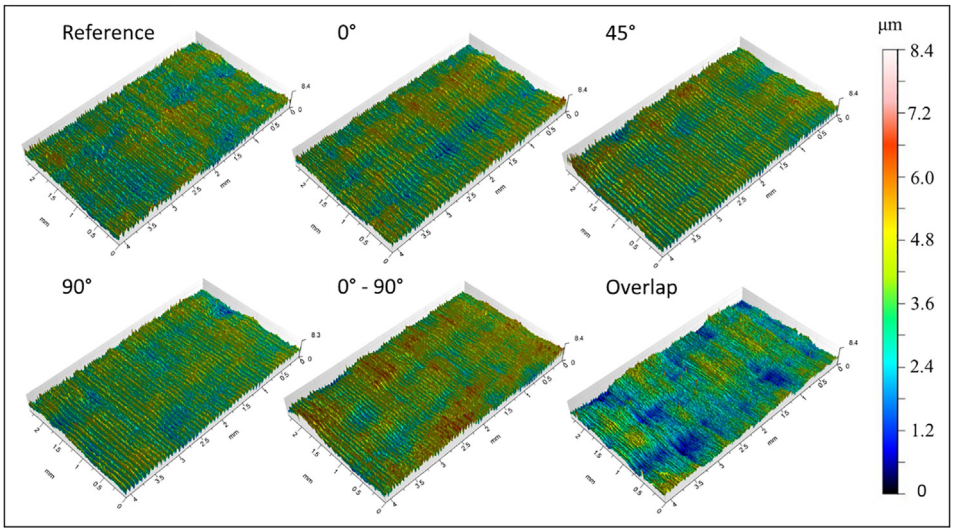

Fig. 9 – Topographies of the machined surfaces with the different tested tools.

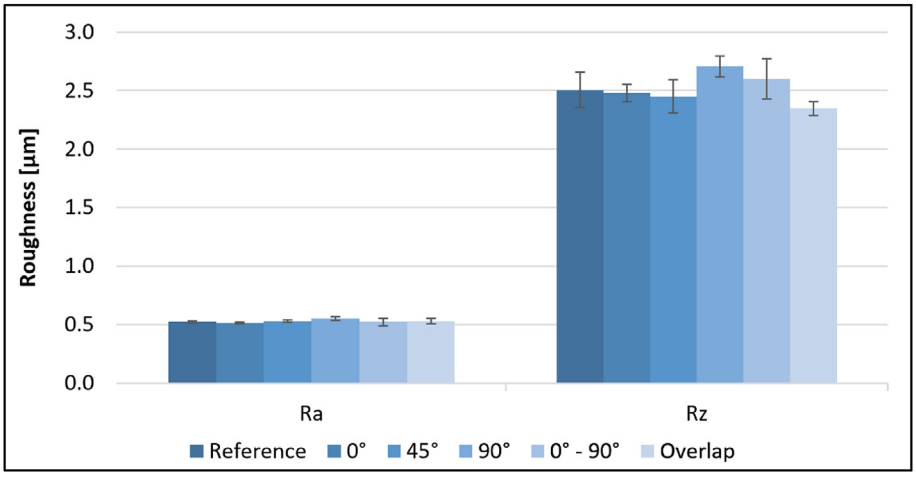

Fig. 10 – Average of the roughness measurements (R_a and R_z) in the final machined surfaces.

force (F_t), feed force (F_f), and the calculated modulus from the three force components in each test is shown.

In the case of the reference insert and the ones provided with chipbreakers with 0° and 45°, respectively cutting forces obtained were similar. This is in accordance with the chip morphology generated in which in these cases also was the same. In particular, taking the modulus of the insert without chipbreaker as a reference, the difference was between 2% and 4%. These values are below 10%; therefore, in these two cases, the chipbreakers did not have an influence on the chip flow and the friction between tool-chip interfaces. On the other hand, in the cases in which 90° and combination of 0°–90° and 0° overlapped were applied to the inserts, an increase of cutting forces are obtained. In comparison with the reference, the increases in the modulus force achieved 45%, 113%, 145%, respectively. In the cases of 90° and 0°-90°combination, the increase was due to the friction between tool-chip interface is enhanced due to the path of the chips through the rake face did not encounter any obstacle which blocks them and obtaining then chip balls. On the other hand, in the case of the chipbreaker overlapped at 0° this increase is caused by the opposite. In particular, the chip-sliding phenomenon is reduced due to chips hitting the chipbreaker frontally and increasing chip curling owing to the increase of the width of the grooves. This fact causes the chip to break and, thus, increasing the magnitude of the cutting forces.

In terms of surface quality, all the machined surfaces presented similar behaviour for all the texturizations (see Fig. 9). Having a look at the literature, some researchers have reported an increase in surface roughness due to texturing [33], whereas decreasing surface roughness was also been observed [45]. In order to evaluate the influence of texturing

Table 3 – ANOVA.

Origin of variations	Sum of squares	Degrees of freedom	Mean squares	F	Probability	Critical F
ANOVA R_a						
Between groups	0.00217428	5	0.000435	1.38734491	0.296316226	3.10587524
Within groups	0.00376133	12	0.000313			
Total	0.00593561	17				
ANOVA R_z						
Between groups	0.23345	5	0.04669	3.09546961	0.05048592	3.10587524
Within groups	0.181	12	0.01508333			
Total	0.41445	17				

on finished workpiece quality, the comparison of surface roughness for different textured tools and their ANOVA analysis was performed.

Fig. 10 shows the average roughness (R_a and R_z) measurements for each machined surface. For measuring settings, a cut-off length of 0.25 mm and an evaluation length of 1 mm were used, according to standard ISO 4288: 1996 [46]. Table 3 shows the ANOVA analysis for both R_a and R_z roughness parameters.

Although there were some small differences in roughness measurements, through the statistical study carried out with ANOVA, it was allowed to establish that texturizations did not have a significant effect on roughness with the cutting parameters used in the tests.

5. Conclusions

In the present work a complete characterization of PCD substrate was carried out to generate by laser texturization (laser beam machining), several chipbreakers in PCD inserts to be applied during Ti6Al4V turning with the aim of obtaining a suitable performance that break chips in a feasible way. The main conclusions obtained from the research carried out are listed below:

- The suitable laser parameters to deal with diamond polycrystalline used in inserts were a scan speed of 400 mm/s and pulse frequency of 50,000 Hz combined with a radial step of 0.02 mm and pulse duration of 250 ns. With these conditions, the average surface roughness obtained in PCD substrate was 1.31 μm and the mean values of five consecutive maximum heights between peak-valley were 19.013 μm, being the most appropriate to be used to generate chipbreakers.
- Regarding the chipbreakers performance, the parallel grooving to the tool edge and the overlapped grooves proved to be reliable for effectively and consistently redirecting chips away from the part. Nevertheless, from the five performances proposed, only with the overlapped 0° strategy a real chip breakage was obtained.
- Chip breakage is a parameter to have taken into account in order to control cutting forces. It should be noted that forcing chip breakage instead of allowing it flow through the rake face implies an increase in cutting forces due to the increase in chip curling generated by the textured surface.
- The analysis of variance carried out established that the final surface roughness achieved in the workpiece surface was not affected by the tested texturizations using a cutting speed of 150 m/min, a feed of 0.05 mm/rev and a depth of cut of 0.25 mm.

Therefore, the use of the correct chipbreaker is a way of obtaining an improvement, which can prevent premature tool failure, and at the same time reducing the chip length with the aim of stabilizing the process. In particular, a chipbreaker parallel (0°) to the cutting edge with overlapping strategy is the best performance to stabilize Ti6Al4V turning process with PCD inserts and consequently achieving a process that can be industrialized for manufacturing of turbomachinery rotary critical components successfully.

Declaration of Competing Interest

The authors declare that they have no known competing financial interests or personal relationships that could have appeared to influence the work reported in this paper.

Acknowledgments

Authors are grateful to Basque government group IT IT1337-19, the Ministry of Mineco REF DPI2016-74845-R and PID2019-109340RB-I00, and the UPV/EHU itself for the financial aid for the pre-doctoral grants PIF 19/96.

REFERENCES

[1] M'Saoubi R, Axinte D, Soo SL, Nobel C, Attia H, Kappmeyer G, et al. High performance cutting of advanced aerospace alloys and composite materials. CIRP Ann – Manuf Technol 2015;64:557–80. https://doi.org/10.1016/j.cirp.2015.05.002.

[2] Williams JC, Starke EA. Progress in structural materials for aerospace systems. Acta Mater 2003;51:5775–99. https://doi.org/10.1016/j.actamat.2003.08.023.

[3] Venkatesan K, Mathew AT, Devendiran S, Ghazaly NM, Sanjith S, Raghul R. Machinability study and multi-response optimization of cutting force, Surface roughness and tool wear on CNC turned Inconel 617 superalloy using Al2O3 Nanofluids in Coconut oil. Elsevier B.V. Procedia Manuf. 2019;30:396–403. https://doi.org/10.1016/j.promfg.2019.02.055.

[4] Zaman HA, Sharif S, Kim DW, Idris MH, Suhaimi MA, Tumurkhuyag Z. Machinability of cobalt-based and cobalt chromium molybdenum alloys - a review. Procedia Manuf 2017;11:563–70. https://doi.org/10.1016/j.promfg.2017.07.150.
[5] Ezugwu EO, Bonney J, Yamane Y. An overview of the machinability of aeroengine alloys. J Mater Process Technol 2003;134:233–53. https://doi.org/10.1016/S0924-0136(02)01042-7.
[6] Suárez A, Veiga F, de Lacalle LNL, Polvorosa R, Wretland A. An investigation of cutting forces and tool wear in turning of Haynes 282. J Manuf Process 2019;37:529–40. https://doi.org/10.1016/j.jmapro.2018.12.025.
[7] Amigo FJ, Urbikain G, Pereira O, Fernández-Lucio P, Fernández-Valdivielso A, de Lacalle LNL. Combination of high feed turning with cryogenic cooling on Haynes 263 and Inconel 718 superalloys. J Manuf Process 2020;58:208–22. https://doi.org/10.1016/j.jmapro.2020.08.029.
[8] Ganguli S, Kapoor SG. Improving the performance of milling of titanium alloys using the atomization-based cutting fluid application system. J Manuf Process 2016;23:29–36. https://doi.org/10.1016/j.jmapro.2016.05.011.
[9] Ulutan D, Ozel T. Machining induced surface integrity in titanium and nickel alloys: a review. Int J Mach Tool Manufact 2011;51:250–80. https://doi.org/10.1016/j.ijmachtools.2010.11.003.
[10] Wei D, Zhang P, Yao Z, Chen X, Li F. Double glow plasma surface Cr-Ni alloying of Ti6Al4V alloys: mechanical properties and impact of preparing process on the substrate. Vacuum 2018;155:233–41. https://doi.org/10.1016/j.vacuum.2018.05.049.
[11] Sun J, Guo YB. A comprehensive experimental study on surface integrity by end milling Ti-6Al-4V. J Mater Process Technol 2009;209:4036–42. https://doi.org/10.1016/j.jmatprotec.2008.09.022.
[12] Pervaiz S, Rashid A, Deiab I, Nicolescu M. Influence of tool materials on machinability of titanium- and nickel-based alloys: a review. Mater Manuf Process 2014;29:219–52. https://doi.org/10.1080/10426914.2014.880460.
[13] Paiva JM, Shalaby MAM, Chowdhury M, Shuster L, Chertovskikh S, Covelli D, et al. Tribological and wear performance of carbide tools with TiB 2 PVD coating under varying machining conditions of TiAl6V4 aerospace alloy. Coatings 2017;7. https://doi.org/10.3390/coatings7110187.
[14] Qi HS, Mills B. Formation of a transfer layer at the tool-chip interface during machining. Wear 2000;245:136–47. https://doi.org/10.1016/S0043-1648(00)00474-9.
[15] Chowdhury MSI, Bose B, Yamamoto K, Shuster LS, Paiva J, Fox-Rabinovich GS, et al. Wear performance investigation of PVD coated and uncoated carbide tools during high-speed machining of TiAl6V4 aerospace alloy. 203168 Wear 2020:446–7. https://doi.org/10.1016/j.wear.2019.203168.
[16] Arulkirubakaran D, Senthilkumar V, Kumawat V. Effect of micro-textured tools on machining of Ti-6Al-4V alloy: an experimental and numerical approach. Int J Refract Met Hard Mater 2016;54:165–77. https://doi.org/10.1016/j.ijrmhm.2015.07.027.
[17] Biksa A, Yamamoto K, Dosbaeva G, Veldhuis SC, Fox-Rabinovich GS, Elfizy A, et al. Wear behavior of adaptive nano-multilayered AlTiN/MexN PVD coatings during machining of aerospace alloys. Tribol Int 2010;43:1491–9. https://doi.org/10.1016/j.triboint.2010.02.008.
[18] Fernández-Abia AI, Barreiro J, Fernández-Larrinoa J, López de Lacalle LN, Fernández-Valdivielso A, Pereira OM. Behaviour of PVD coatings in the turning of austenitic stainless steels. Elsevier Ltd Procedia Eng. 2013;63:133–41. https://doi.org/10.1016/j.proeng.2013.08.241.
[19] Berg G, Friedrich C, Broszeit E, Berger C. Development of chromium nitride coatings substituting titanium nitride. Surf Coating Technol 1996;86–87:184–91. https://doi.org/10.1016/S0257-8972(96)03042-3.
[20] Lupicka O, Warcholinski B. The adhesion of CrN thin films deposited on modified 42CrMo4 steel. Ann Mater Sci Eng 2017;2017. https://doi.org/10.1155/2017/4064208.
[21] Milošev I, Strehblow HH, Navinšek B. Comparison of TiN, ZrN and CrN hard nitride coatings: electrochemical and thermal oxidation. Thin Solid Films 1997;303:246–54. https://doi.org/10.1016/S0040-6090(97)00069-2.
[22] Kuram E. The effect of monolayer TiCN-, AlTiN-, TiAlN-and two layers TiCN + TiN- and AlTiN + TiN-coated cutting tools on tool wear, cutting force, surface roughness and chip morphology during high-speed milling of Ti6Al4V titanium alloy. Proc Inst Mech Eng Part B J Eng Manuf 2018;232:1273–86. https://doi.org/10.1177/0954405416666905.
[23] Fernández-Valdivielso A, López de Lacalle L, Fernández-Lucio P, González H. Turning of austempered ductile Iron with ceramic tools. Proc Inst Mech Eng Part B J Eng Manuf 2020:095440542095715. https://doi.org/10.1177/0954405420957154.
[24] Tan DW, Guo WM, Wang HJ, Lin HT, Wang CY. Cutting performance and wear mechanism of TiB2-B4C ceramic cutting tools in high speed turning of Ti6Al4V alloy. Ceram Int 2018;44:15495–502. https://doi.org/10.1016/j.ceramint.2018.05.209.
[25] Silva RBD, Machado Á, Ezugwu EO, Bonney J. Evaluation of the machinability of Ti-6Al-4V alloy with (SiCW) whisker reinforced alumina ceramic cutting tool under various cooling environments. 2005.
[26] López De Lacalle LN, Pérez-Bilbatua J, Sánchez JA, Llorente JI, Gutiérrez A, Albóniga J. Using high pressure coolant in the drilling and turning of low machinability alloys. Int J Adv Manuf Technol 2000;16:85–91. https://doi.org/10.1007/s001700050012.
[27] Corduan N, Himbert T, Poulachon G, Dessoly M, Lambertin M, Vigneau J, et al. Wear mechanisms of new tool materials for Ti-6Al-4V high performance machining. CIRP Ann - Manuf Technol 2003;52:73–6. https://doi.org/10.1016/S0007-8506(07)60534-4.
[28] Oliaei SNB, Karpat Y, Davim JP, Perveen A. Micro tool design and fabrication: a review. J Manuf Process 2018;36:496–519. https://doi.org/10.1016/j.jmapro.2018.10.038.
[29] Sales WF, Schoop J, Jawahir IS. Tribological behavior of PCD tools during superfinishing turning of the Ti6Al4V alloy using cryogenic, hybrid and flood as lubri-coolant environments. Tribol Int 2017;114:109–20. https://doi.org/10.1016/j.triboint.2017.03.038.
[30] Sadik MI, Coronel E, Lattemann M. Influence of characteristic properties of PCD grades on the wear development in turning of β-titanium alloy (Ti5Al5V5Mo3Cr). Wear 2019;426–427:1594–602. https://doi.org/10.1016/j.wear.2019.01.012.
[31] Oosthuizen GA, Akdogan G, Treurnicht N. The performance of PCD tools in high-speed milling of Ti6Al4V. Int J Adv Manuf Technol 2011;52:929–35. https://doi.org/10.1007/s00170-010-2804-2.
[32] Richards N, Aspinwall D. Use of ceramic tools for machining nickel based alloys. Int J Mach Tool Manufact 1989;29:575–88. https://doi.org/10.1016/0890-6955(89)90072-2.
[33] Xing Y, Deng J, Zhao J, Zhang G, Zhang K. Cutting performance and wear mechanism of nanoscale and microscale textured Al2O3/TiC ceramic tools in dry cutting of hardened steel. Int J Refract Met Hard Mater 2014;43:46–58. https://doi.org/10.1016/J.IJRMHM.2013.10.019.
[34] Cui X, Guo Z, Guo J. Intermittent turning performance of ceramic tools with surface micro-geometry designed considering fluid-like behavior of chip. Ceram Int

2018;44:16890–9. https://doi.org/10.1016/j.ceramint.2018.06.127.

[35] Rajbongshi SK, Annebushan Singh M, Kumar Sarma D. A comparative study in machining of AISI D2 steel using textured and non-textured coated carbide tool at the flank face. J Manuf Process 2018;36:360–72. https://doi.org/10.1016/j.jmapro.2018.10.041.

[36] Mishra SK, Ghosh S, Aravindan S. Performance of laser processed carbide tools for machining of Ti6Al4V alloys: a combined study on experimental and finite element analysis. Precis Eng 2019;56:370–85. https://doi.org/10.1016/j.precisioneng.2019.01.006.

[37] Wu M, Yu A, Chen Q, Wang Y, Yuan J, Sun L, et al. Design of adjustable chip breaker for PCD turning tools. Int J Mech Sci 2020;172:105411. https://doi.org/10.1016/j.ijmecsci.2019.105411.

[38] Tamil Alagan N, Zeman P, Hoier P, Beno T, Klement U. Investigation of micro-textured cutting tools used for face turning of alloy 718 with high-pressure cooling. J Manuf Process 2019;37:606–16. https://doi.org/10.1016/j.jmapro.2018.12.023.

[39] Everson C, Molian P. Fabrication of polycrystalline diamond microtool using a Q-switched Nd:YAG laser. Int J Adv Manuf Technol 2009;45:521–30. https://doi.org/10.1007/s00170-009-1999-6.

[40] Pacella M, Nekouie V, Badiee A. Surface engineering of ultra-hard polycrystalline structures using a nanosecond Yb fibre laser: effect of process parameters on microstructure, hardness and surface finish. J Mater Process Technol 2019;266:311–28. https://doi.org/10.1016/j.jmatprotec.2018.11.014.

[41] Patel K, Liu G, Shah SR, Özel T. Effect of micro-textured tool parameters on forces, stresses, wear rate, and variable friction in titanium alloy machining. J Manuf Sci Eng Trans ASME 2020;142. https://doi.org/10.1115/1.4045554.

[42] Kumar Mishra S, Ghosh S, Aravindan S. Machining performance evaluation of Ti6Al4V alloy with laser textured tools under MQL and nano-MQL environments. J Manuf Process 2020;53:174–89. https://doi.org/10.1016/J.JMAPRO.2020.02.014.

[43] Iqbal SA, Mativenga PT, Sheikh MA. A comparative study of the tool-chip contact length in turning of two engineering alloys for a wide range of cutting speeds n.d. https://doi.org/10.1007/s00170-008-1582-6.

[44] Grzesik W, Kwiatkowska E. An energy approach to chip-breaking when machining with grooved tool inserts. Int J Mach Tool Manufact 1997;37:569–77. https://doi.org/10.1016/S0890-6955(96)00076-4.

[45] Zhang K, Deng J, Ding Z, Guo X, Sun L. Improving dry machining performance of TiAlN hard-coated tools through combined technology of femtosecond laser-textures and WS2 soft-coatings. J Manuf Process 2017;30:492–501. https://doi.org/10.1016/J.JMAPRO.2017.10.018.

[46] Standard I. ISO – ISO 4288:1996/Cor 1:1998 – geometrical product specifications (GPS) — surface texture: profile method — rules and procedures for the assessment of surface texture — technical corrigendum 1. n.d, https://www.iso.org/standard/29875.html. [Accessed 15 June 2021].